



## Oral insulin delivery using P(MAA-g-EG) hydrogels: effects of network morphology on insulin delivery characteristics

Koji Nakamura<sup>a</sup>, Robert J. Murray<sup>a</sup>, Jeffrey I. Joseph<sup>b</sup>, Nicholas A. Peppas<sup>c</sup>,  
Mariko Morishita<sup>d</sup>, Anthony M. Lowman<sup>a,\*</sup>

<sup>a</sup>Department of Chemical Engineering, Drexel University, 3141 Chestnut Street, Philadelphia, PA 19104, USA

<sup>b</sup>The Artificial Pancreas Center, Department of Anesthesiology, Thomas Jefferson University, Philadelphia, PA, USA

<sup>c</sup>Departments of Chemical and Biomedical Engineering, University of Texas, Austin, TX, USA

<sup>d</sup>Department of Pharmaceutics, Hoshi University, Tokyo, Japan

Received 9 September 2003; accepted 31 December 2003

### Abstract

Hydrogels of poly(methacrylic acid-g-ethylene glycol) were prepared using different reaction water contents in order to vary the network mesh size, swelling behavior and insulin loading/release kinetics. Gels prepared with greater reaction solvent contents swelled to a greater degree and had a larger network mesh size. All of the hydrogels were able to incorporate insulin and protected it from release in acidic media. At higher pH (7.4), the release rates increased with reaction solvent content. Using a closed loop animal model, all of the insulin loaded formulations produced significant insulin absorption in the upper small intestine combined with hypoglycemic effects. In these studies, bioavailabilities ranged from 4.6% to 7.2% and were dependent on reaction solvent content.

© 2004 Elsevier B.V. All rights reserved.

**Keywords:** Hydrogels; Complexation; Oral protein delivery; Insulin

### 1. Introduction

Generally, peptides and proteins such as insulin cannot be administered via the oral route because of the degradation by the proteolytic enzymes in the gastrointestinal tract and the extremely slow rate of transport across the mucosal membrane. In order to overcome these hurdles to effective oral protein delivery, several strategies have been employed, such as the use of absorption enhancers [1–3], enzyme inhib-

itors [4,5], enteric coatings [6,7], and nanoparticle delivery [8]. Recently, nanoparticulate delivery systems have been studied because the incorporated protein and peptide-drugs could be protected from degradation in the gastrointestinal mucosa, and the attachment of ligands such as lectin on their surface provided for targeted delivery to specific GI segments (for absorption) because the lectin specifically interacts with the mucus layer, particularly glycoproteins [9,10]. However, the permeation of nanoparticles across the mucosa was still small (less than 10%), resulting in poor bioavailability of the drug and plasma drug levels below the therapeutic levels [11,12]. The use of protease inhibitors [4,5] and absorption

\* Corresponding author. Tel.: +1-215-895-2228; fax: +1-215-895-5837.

E-mail address: [alowman@drexel.edu](mailto:alowman@drexel.edu) (A.M. Lowman).

enhancers [1–3] have led to improved uptake of protein drugs, however, these agents are not specific and could aid in the uptake of other undesirable proteins or peptides in the GI tract.

A new class of complexation hydrogels comprised of poly(ethylene glycol) (PEG) chains grafted on poly(methacrylic acid) (PMAA) backbone chain, henceforth designated as P(MAA-g-EG) have shown promise as oral delivery vehicles for insulin [13–17]. These complexation hydrogels are suitable candidate for the oral delivery of proteins or peptides due to their abilities to respond to changes in pH in the GI tract and provide protection to the drugs from the harsh environment of the GI tract. In this hydrogel, the structure of network exhibits pH-responsive swelling and changes in network pore structure due to the reversible formation/dissociation of interpolymer complexes [15]. At low pH, similar to the environment of the stomach, these interpolymer complexes form due to hydrogen bonding between the carboxylic acid protons of PMAA and the oxygen in the PEG chains. These complexes function as temporary physical crosslinks that can entrap and protect drugs in the network structure. In higher pH media (greater than 5.2) such as that found in the upper small intestine, the complexes dissociate due to ionization of the pendant acid groups and the network swells to a significantly large degree.

In addition to the complexation behavior, these gels are promising candidates for oral protein delivery because they have the capability to entrap and release insulin efficiently as well as enhance transport across the intestinal mucosa [13,16,17]. It has previously been reported that the insulin incorporation efficiency into these hydrogels was greater than 90% and that the insulin could be protected in simulated gastric fluid (pH=1.2) and released in simulated intestinal fluid (pH 7.4) [16]. The oral administration of insulin loaded complexation polymer provided for significant insulin absorption and glucose reduction in healthy and diabetic rats [13]. Moreover, P(MAA-g-EG) hydrogels induced a decrease in mucosal membrane resistance in Caco-2 monolayers, without any appreciable cytotoxicity [17]. This previous work clearly demonstrated the potential of P(MAA-g-EG) carriers for oral insulin delivery.

In previous studies using complexation hydrogels, the insulin release from the polymeric microparticles

was fairly rapid—nearly complete in 1 h swelling in phosphate buffer solution (pH=7.4) [16]. This rapid *in vitro* release would translate to a burst release in the upper small intestine and potentially degradation of some insulin before absorption. Here, the morphology of the P(MAA-g-EG) networks was modified by altering the solvent content during network formation. Through modifications of the network morphology, the insulin release characteristics can be tailored in such a way that may improve oral bioavailability of the insulin. Specifically, in this work the effects of solvent reaction content on network structure, *in vitro* insulin loading and release kinetics and *in vivo* efficacy of the delivery vehicles in a closed-loop absorption model have been evaluated.

## 2. Materials and methods

### 2.1. Materials

Methacrylic acid (MAA) and insulin (bovine and human) were purchased from Sigma (St. Louis, MO). Dimethoxy propyl acetophenone (DMPA) was purchased from Aldrich (Milwaukee, WI). In this study, MAA was purified by passing it through a column packed with DE-HIBIT 200 (Polysciences, Warrington, PA) in order to remove the inhibitor. Methoxy terminated poly(ethylene glycol) monomethacrylate 1000 (PEGMA), and tetraethylene glycol dimethacrylate (TEGDMA) were purchased from Polysciences.

### 2.2. Hydrogel synthesis

Microparticles of P(MAA-g-EG) were prepared by free-radical, solution photo-polymerization of MAA and PEGMA [16]. The monomers were mixed in appropriate molar ratios to yield a 1:1 ratio of MAA/EG units in the gel. The solutions were diluted to 22.3% (polymer I), 44.7% (polymer II) or 67.0% (polymer III) (wt./wt.) of the total monomers with a 1:1 (vol./vol.) mixture of ethanol/water. TEGDMA was added as a crosslinking agent in the amount of  $X=0.075$  moles TEGDMA per MAA. DMPA was added as initiator in the amount of 1% weight of the monomers.

The reaction mixture was pipetted between glass plates spaced 0.8 mm apart, creating a monomer film.

The reaction was initiated by exposing the monomer film to UV light (Ultracure 100, Efos, Buffalo, NY) at  $1 \text{ mW/cm}^2$  at 365 nm for 30 min. The ensuing hydrogels were removed from the glass plates and rinsed for 1 week in DI-water (changed daily) to remove the unreacted monomers and the sol fraction.

### 2.3. Hydrogel swelling

Polymer discs (diameter = 14 mm) were cut from the films and dried to a constant weight under vacuum at  $37^\circ\text{C}$ . The dry polymers were weighed in air and heptane in order to determine the dry volume of the disc using a buoyancy technique [15]. The dry discs were individually placed in 20 ml phosphate-buffered saline solutions of varying pH at  $37^\circ\text{C}$ . The mass and weights of the swollen polymer discs were recorded as function of time for 12 h of swelling. The volume swelling ratio,  $Q$ , was determined as the volume of swollen gel/volume of dry polymer and the weight swelling ratio,  $q$ , was calculated at the weight of the swollen gel/weight of the dry polymer. In order to determine the equilibrium water content, the gels were allowed to equilibrate in the solutions for 1 week with the solution being changed daily. The equilibrium water fraction in the gel was calculated as  $1 - 1/q$ . Additionally, dynamic swelling studies were performed in which the polymers were swollen in solutions of set pH for a specified time period and then transferred to a different pH solution in order to evaluate how fast the polymers could respond to changes in pH.

### 2.4. Characterization of network structure

Rubber elasticity experiments were performed using an automated materials tensile testing system (Instron Model 4442, Park Ridge, IL) to characterize the network structure of the hydrogels. The dry polymer films were allowed to swell to equilibrium in solutions of varying pH at  $37^\circ\text{C}$ . Swollen polymers were cut into strips to yield specimens of length,  $l_0$ , 25 mm and width,  $w$ , of 2 mm. The sample thickness,  $2\delta$ , was dependent on the pH of the swelling agent. The samples were positioned in the grips and covered with a thin layer of high viscosity mineral oil to prevent solvent loss. The samples were elongated at 2 mm/min until the hydrogels reached a

maximum elongation of 10%. The stress strain behavior of the swollen network was observed.

### 2.5. Insulin loading

For the insulin loading, the dry polymer films were pulverized and crushed into fine microparticles using a coffee grinder. The particles were ground for sufficient time to generate particles that could pass through sieves with a mesh size of  $43 \mu\text{m}$ . All of the glassware used for these experiments was siliconized by treatment with Sigmacote® (Sigma). Insulin loading was achieved by dissolving 10 mg of bovine insulin in 20 ml PBS (pH = 7.4). The crushed microparticles (140 mg) were dispersed in this insulin solutions at  $37^\circ\text{C}$  and stirred at 300 rpm. At set intervals, 1 ml samples were withdrawn from the solution using syringes equipped with  $0.45 \mu\text{m}$  membrane filters. After 6 h, 10 ml of 0.1N HCl was added to the solutions to collapse the polymers. These solutions were filtered with cellulose acetate/cellulose nitrate filter ( $0.45 \mu\text{m}$ , Fisher Science, PA). The polymers were further washed with 100 ml of 0.1 N HCl and 100 ml of DI-water. The insulin-loaded polymer (ILP) was dried under vacuum at  $37^\circ\text{C}$ .

HPLC was used to determine the insulin concentration in the samples as well as the wash solution [16]. Briefly, a Waters Symmetry® 300 column (C18,  $300\text{\AA}$ ,  $5 \mu\text{m}$ ,  $4.6 \times 250 \text{ mm}$ ) was used with a mixture of acetonitrile/water including 0.1% TFA (30:70, vol./vol.) employed as the mobile phase. Samples ( $20 \mu\text{l}$ ) were injected to Waters 2690 separations module equipped with a 996 Photodiode Array detector at a 1 ml/min flow rate. The incorporation efficiency was determined based on the amount of insulin present in the loading and three wash solutions.

### 2.6. Insulin release from ILPs

The insulin release studies were performed using siliconized vessels. In these experiments, 10 mg of ILP were dispersed in 20 ml PBS (of varying pH) at  $37^\circ\text{C}$ . The solutions were stirred at 300 rpm and 1 ml aliquots were withdrawn using syringe equipped with membrane filter at set intervals. To maintain constant volume, 1 ml of fresh PBS warmed at  $37^\circ\text{C}$  was added after each sample was withdrawn. The insulin

concentration in the release solutions was determined using HPLC.

### 2.7. Closed-loop intestinal absorption studies

For the animal studies, human recombinant insulin was incorporated into the polymers. Loading and release studies were performed to confirm that the degree of loading and release behavior were not different from bovine insulin. In these experiments, male Sprague–Dawley rats, weighing approximately 180 g, were fasted for 24 h prior to the administration of the ILP. The rats were anesthetized by i.p. injection of pentobarbital (50 mg/kg). The body temperature of the animals was maintained near 37 °C using a neonatal warming light.

In this study, the in situ loop method was employed [18]. Briefly, a front middle incision was made in the abdomen and ileal segment was isolated. A 10 cm of the isolated segment was washed with 20 ml PBS at 37 °C and then the abdomen was clamped. The glucose levels were allowed to stabilize for 1 h after surgery. The formulations (containing a 25 IU/kg dose) were suspended in 0.3 ml PBS in a syringe and infused into a 7-cm ileal segment. In order to ensure that all of the ILP was delivered, the syringe was twice washed with 0.2 ml of warmed PBS and injected into the ileal segment.

Blood samples were withdrawn from jugular vein immediately prior to the administration of the ILP as the  $t=0$  value, and at 5, 10, 15, 30, 60, 120, 180, and 240 min post administration of the formulations. After taking blood samples, glucose levels were determined using a HemoCue blood glucose analyzer (HemoCue, Angelholm, Sweden). The serum was collected by the centrifugation of the blood samples at 13,000 rpm for 3 min. The serum was stored in freezer at –20 °C until analysis of insulin. The insulin levels were determined by an enzyme immunoassay (Alpco Research).

To determine the pharmacological bioavailability and absolute bioavailability of insulin, rats received subcutaneous insulin injections and the glucose level and insulin concentration were monitored. The area above the curve of glucose (AAC) and the area under the curve of insulin (AUC) were calculated for each dosage form. The pharmacological bioavailability and absolute bioavailability of insulin was determined as the ratio of the AAC (pharmacological) or AUC

(absolute) for direct intestinal administration divided by the AAC (pharmacological) or AUC (absolute) for subcutaneous injections. The mean residence time (MRT) was calculated by dividing the AUMC by  $AUC_{\text{insulin}}$ , where AUMC is the area under the first moment curve for insulin for the first 3 h.

### 2.8. Statistical analysis

Each value was expressed as the mean  $\pm$  S.D. For group comparisons, the one-way layout analysis of variance (ANOVA) with duplication was applied. Significant differences in the mean values were evaluated by the Student's unpaired *t*-test. A *p* value of less than 0.05 was considered to be significant.

## 3. Results and discussion

Previously, it has been reported that complexation polymers of P(MAA-g-EG) demonstrated appropriate release characteristics for oral insulin delivery based on in vitro release studies [16] and that the oral administration of this insulin loaded polymer could significantly reduce the blood glucose levels in healthy and diabetic rats [16,18]. However, in previous studies, the focus was on one P(MAA-g-EG) formulation that provided for extremely rapid insulin release in intestinal fluid. Therefore, the focus of this work was to prepare the complexation gels with varied network pore structure by changing of the mixing ratio of solvent to monomer during polymerization and to evaluate how the changes of pore morphology affected the properties of the gels with respect to swelling, insulin incorporation, in vitro release kinetics, and hypoglycemic effect following direct intestinal administration using a closed-loop model. In this study, three different polymers were prepared by changing mixing ratio of ethanol/water to monomers (polymer I: 22.3%, polymer II: 44.4%, polymer III: 66.3%). Polymer II is the same formulation as one reported previously [13,16,18].

### 3.1. Hydrogel swelling

Dynamic and equilibrium swelling studies were performed to confirm whether the new complexation polymers exhibited similar pH-responsive swelling

behavior as seen previously. Dynamic swelling studies were performed to see how the polymers responded to changes in environmental pH. As seen in Fig. 1, the polymers did not swell when swollen in pH=1.2 or 5.0 media (representing the range of stomach pH values in various states), however, when they were transferred into pH=7.4 solutions after 3 h (simulating gastric emptying), the gels swelled rapidly. The rate at which the polymers swelled in the higher pH solution was dependent on the reaction water content. Gels prepared with higher water contents swelled faster. Furthermore, when the pH of solution was decreased to 1.2, all of the gels collapsed rapidly. These data implied that these polymers could respond to changes in pH of the surrounding media in a manner similar to what has previously been reported [13–16].

The swelling behavior of the three formulations is shown in Fig. 2 for longer time periods, as a function of solution pH. As expected, none of the gels swelled significantly in pH=1.2 or 5.0 solutions due to the formation of complexes at this pH. For each system, the equilibrium-swelling ratio was less than 1.2, which is equivalent to water contents of approximately 15% or less. However, in the higher pH solution

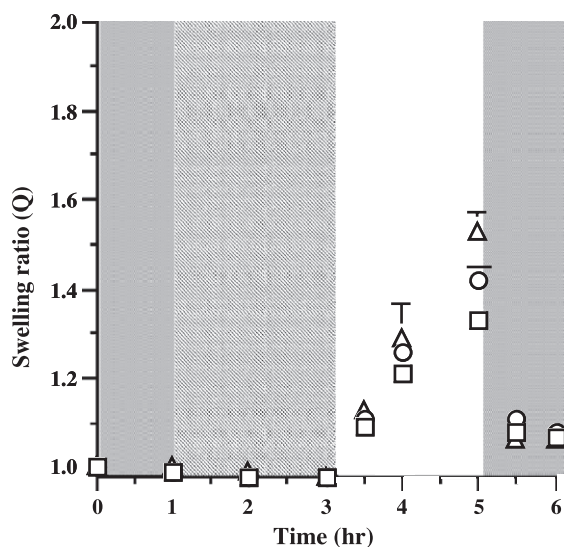


Fig. 1. Dynamic swelling behavior of polymer I (□), polymer II (○) and polymer III (△) at 37 °C in solutions of pH=1.2 (■), pH=5.0 (▨), pH=7.4 (□). Each data point represents the mean  $\pm$  S.D. ( $n=3$ ).

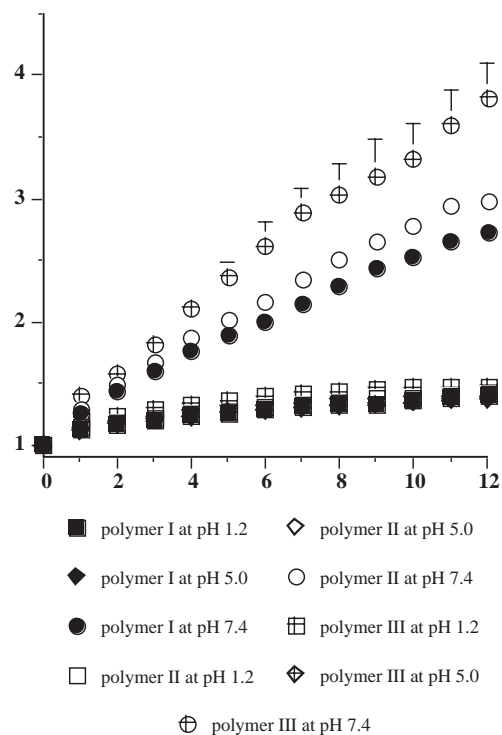


Fig. 2. Swelling behavior of complexation polymers at 37 °C. Each data point represents the mean  $\pm$  S.D. ( $n=3$ ).

(7.4), all of the polymers swelled rapidly during the 12-h period. The polymer prepared with the greatest water content (polymer III) swelled to the highest degree at 12 h and had the highest equilibrium water content (97%). Polymer II swelled faster than polymer I in the 12 h and had higher equilibrium water content than polymer I (95% for polymer II and 91% for polymer I).

The relative high degrees of polymer swelling was due to the fact that these complexes begin to dissociate in solutions of pH>5.0 [15]. As these physical crosslinks dissolved, the polymer chains could expand and incorporate water into the network due to electric repulsion from the ionization of carboxylic groups and an increased ionic swelling force [15]. The degree to which the gels swelled was increased with increasing solvent content during the synthesis procedure. Despite the fact that the hydrogels were prepared with the same amount of crosslinking agent, it is likely that the reaction solvent content had effects on the network morphology and could have affected the network

mesh size and hence degree of swelling at higher pH values.

### 3.2. Mesh size analysis

Rubber elasticity experiments were performed to calculate the network mesh size as a function of pH and to verify that greater solvent fractions during polymerization caused an increase in network mesh size. For the design of hydrogels in biomedical applications, it is important to control the swelling, diffusion, and mechanical properties. These factors are a function of network mesh size, which may be strongly affected by solvent concentration during polymerization. An increase in solvent concentration will result in the dilution of monomer molecules and free radicals in the bulk solution, which reduces the rate of consumption of these units. Consequently, the propagation rate decreases causing the molecular weight between crosslinks to increase and reduces the degree of crosslinking. Additionally, greater primary cyclization occurs with the increase of solvent concentration. As the propagation rate decreases, the apparent local radical concentration decreases slowly, increase the probability of encountering the pendant double bonds, causing more cyclization [19,20]. Therefore, greater solvent concentrations during the polymerization process leads to increases in the molecular weight between crosslinks and hence greater network mesh sizes.

In order to characterize the effects of solvent content during polymerization on the structure of the complexation networks, rubber elasticity experiments were performed. In these experiments, the tensile stress,  $\tau$ , was calculated from the experiments as the force per cross sectional area of the unstretched, unswollen polymer sample. The elongation,  $\alpha$ , was calculated as the length at any time divided by the initial length of the polymer sample. Based on the theory of rubber elasticity, the tensile modulus,  $G$ , is related to degree of swelling by the following expression [20,21]:

$$\frac{\tau}{\alpha - 1/\alpha^2} = Gv_{2,s}^{-1/3} \quad (1)$$

where  $v_{2,s}$  is the equilibrium polymer volume fraction in the gel ( $1/Q_{eq}$ ). From the moduli of the hydrogel,

the effective molecular weight between crosslinks,  $\bar{M}_e$ , could be calculated for the gels using Eq. (2) as described previously [15,21,22]:

$$\frac{\tau}{\alpha - \alpha^{-2}} = RT\rho_{2,r} \left( \frac{1}{\bar{M}_e} - \frac{1}{\bar{M}_n} \right) \left( \frac{v_{2,s}}{v_{2,r}} \right)^{1/3} \quad (2)$$

In the expression,  $\rho_{2,r}$  and  $v_{2,r}$  represent the density of the polymer and the polymer volume fraction after crosslinking but before swelling (the relaxed state), respectively. The term,  $\bar{M}_n$ , is the number average molecular weight of the linear polymer chains of the copolymer that would have formed without the addition of crosslinker. In previous work, this theoretical value has been calculated as 11,550 for these gels [15]. Using these data, the network correlation length or mesh size,  $\xi$ , was calculated as a function of pH by determining the end-to-end distance of the swollen polymer chains between crosslinks, both covalent and physical using the following equation [15].

$$\xi = \left( \frac{2C_n \bar{M}_e}{M_0} \right)^{1/2} l v_{2,s}^{-1/3} \quad (3)$$

where  $C_n$  is the Flory polymer characteristic ratio determined to be 14.6,  $l$  is the carbon–carbon double bond length (1.54 Å), and  $M_0$  is the molecular weight of the repeating units making up the polymer chains.

The effect of swelling solution pH and solvent concentration during polymerization on the network mesh size is shown in Fig. 3. For all samples, the network mesh size increased dramatically in solutions of pH greater than 5. In the solution with low pH, the gels were complexed and mesh sizes of the networks were similar (63 to 71 Å). It is notable that for all three gels, the mesh sizes were similar in the complexed state that would indicate that the total crosslinking, both physical and chemical, was similar in these states. Previously, it was shown that such a mesh size was sufficient to entrap insulin [13–16]. However, in solutions of pH greater than 5, the mesh sizes were increased dramatically as the complexes dissociated. In the higher pH solutions, gels polymerized at higher solvent fractions had an increased mesh size, which would indicate that the length of the chains between crosslinks could extend further. Clearly, the ratio of mesh size between the two states (complexed/uncomplexed) could be controlled by the solvent

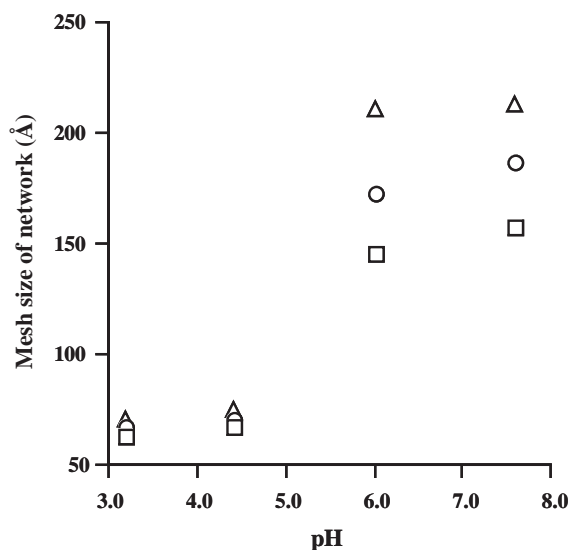


Fig. 3. Hydrogel mesh size as a function of pH at 37 °C for polymer I (□), polymer II (○) and polymer III (△). Each data point represents the mean  $\pm$  S.D. ( $n=3$ ).

concentration during polymerization and thus it was expected that the insulin loading and release kinetics would also be affected by the solvent concentration during polymerization.

### 3.3. Insulin incorporation

Insulin was incorporated into the polymer structures by soaking crushed microparticles of the dry polymers in concentrated insulin solutions (pH=7.4). The uptake of insulin into gels is shown in Fig. 4. Overall, all of the polymers had sufficient large pore sizes to incorporate a significant amount of insulin into the swollen networks. Insulin loading was very rapid in polymers II and III, with greater than 95% of the insulin in the solution partitioning into the gels within 1 h. Loading into polymer I (prepared with the least amount of solvent) was much slower compared with the other gels with the incorporation amount being only 80% at 1 h. However, after 6 h, the incorporation efficiency reached nearly 95%. This difference can be explained by the rates at which the polymers swell. As seen in Fig. 2, polymer I swelled at a much slower rate than the other polymers and had a much smaller mesh size overall, therefore the rate of penetration of insulin into the gels was slower.

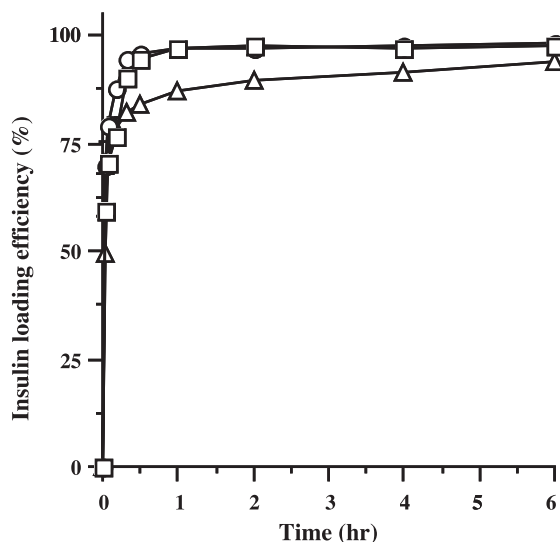


Fig. 4. Insulin incorporation efficiency for polymer III (□), polymer II (○) and polymer I (△) at 37 °C in PBS of pH=7.4. Each data point represents the mean  $\pm$  S.D. ( $n=4$ ).

Following 6 h of loading, HCl was added to the solutions to collapse the polymer and entrap the insulin in the complexed networks. The effects of the collapse of insulin loading are shown in Fig. 5. The treatment of HCl induced the reduction of insulin incorporation efficiency into polymer compared with

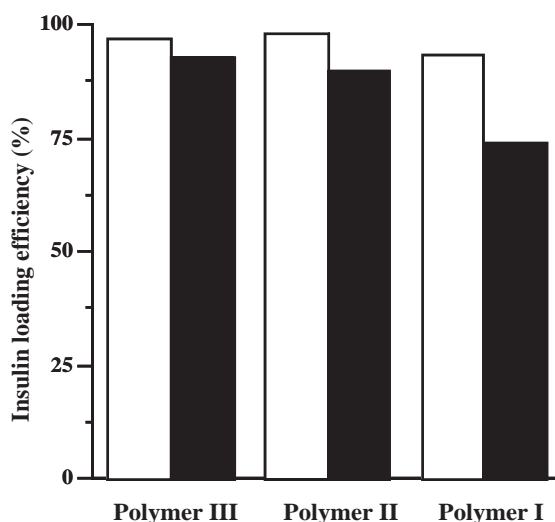


Fig. 5. Insulin loading efficiency for the complexation polymers before (□) and after (■) HCl treatment ( $n=4$ ).

that prior to HCl in the loading solution (polymer III:  $97.3 \pm 0.5\%$  to  $93.0 \pm 1.0\%$ , polymer II:  $98.0 \pm 0.3\%$  to  $90.0 \pm 0.7\%$ , polymer I:  $93.7 \pm 0.3\%$  to  $73.9 \pm 0.7\%$ ). Clearly the most significant reduction was seen in polymer I. The possible reason for the reduction of insulin loading efficiency after treatment of HCl may be due to the elimination of water from polymer. As shown in Fig. 1, the polymers used in this study immediately collapsed in response to a decrease in the pH of the surrounding medium to acidic conditions. However, as polymer I was the slowest swelling polymer it is possible that the gel had not completely equilibrated and the rapid convection of water upon network collapse could have caused the insulin to be squeezed from the polymer.

### 3.4. *In vitro* insulin release

After the ILPs were dried, the particles were dispersed in sufficient quantities of solution to ensure that sink conditions were maintained throughout the experiments. At set points following dispersion in solution, the solutions were assayed for insulin using HPLC. A plot of the fractional insulin release, denoted as the amount released at a given time divided by the theoretical maximum amount released, is shown in Fig. 6. It should be noted that these curves only represent the release behavior of insulin from the ILPs in PBS of pH=7.4 because no insulin was released from any of the samples placed in pH=1.2 or 5.0 solutions. This finding is significant as insulin degradation in the stomach is one of the main barriers for the development of effective oral delivery vehicles for insulin. All of the formulations tested can provide the desired protective effect by no allowing insulin to be released in the stomach where it is readily destroyed by digestive enzymes. In the PBS solutions of pH=7.4, the release of insulin from all of the samples was quite rapid. It is significant to note that insulin release profiles match up well with the dynamic swelling off the polymers as the rate of release was fastest with polymer III and slowest for polymer I.

In prior studies, the composition of the P(MAA-g-EG) gels with respect to MAA/EG ratio was varied in order to attempt to control the release behavior of insulin and found that samples that did not contain 1:1 (mole) of MAA/EG would release significant amounts of insulin in acidic media [14,16]. However, here a set

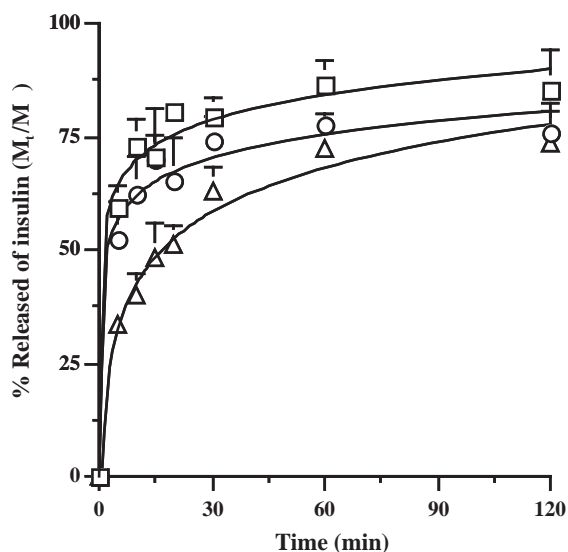


Fig. 6. Insulin release behavior from polymer III ( $\square$ ), polymer II ( $\circ$ ) and polymer I ( $\triangle$ ) at 37 °C in PBS of pH=7.4. Each data represents the mean  $\pm$  S.D. ( $n=4$ ).

of gels has been synthesized that provides the desired protective effect in acidic media and that also allow for tailoring of the release profile in media of pH similar to the intestines. To further evaluate the efficacy of these materials, *in vivo* experiment were performed to determine if the ILPs could provide varied absorption profiles.

### 3.5. Pharmacological effect following intestinal administration of ILP

In this study, an *in situ* closed-loop method was employed to investigate the pharmacological efficacy of ILP following direct administration of the ILP to intestinal segments of rats. Previously, it was found that the ILP with particle sizes of less than 43  $\mu\text{m}$  showed the greatest hypoglycemic effect as compared with larger size ILP particles [18], therefore, all of loaded polymers were sieved through a 43  $\mu\text{m}$  mesh prior to administration.

The glucose response and insulin absorption profiles following the intestinal administration of ILPs to rats at a dose of 25 IU/kg is shown in Fig. 7. In this study, the control sample is the polymer without insulin as numerous prior studies with insulin solutions as a control have shown that no hypoglycemic

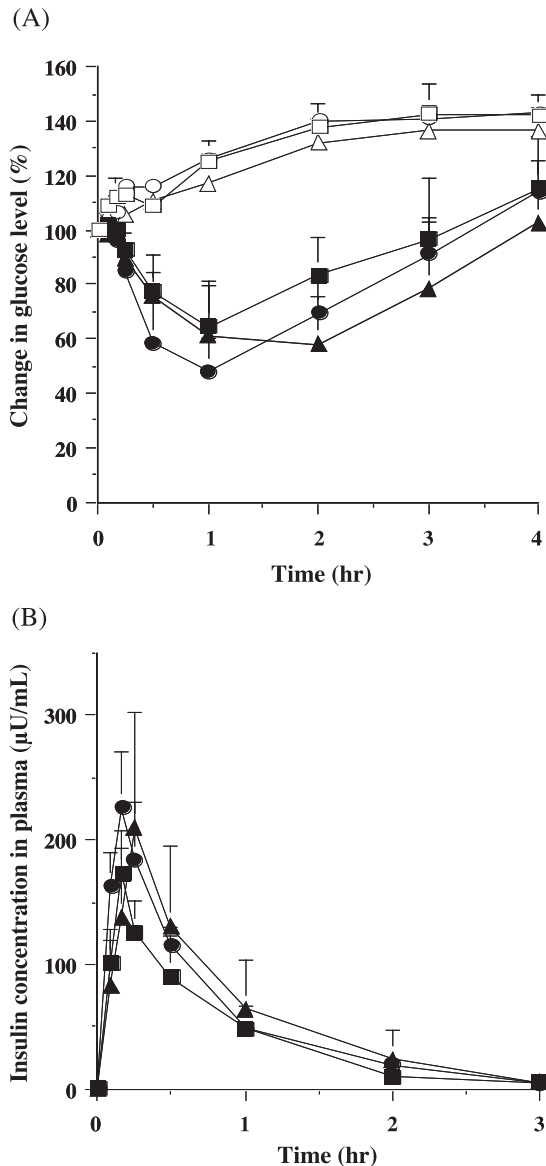


Fig. 7. Serum glucose and insulin levels following the intestinal administration of polymer III (■), polymer II (●) and polymer I (▲) to rats at a dose of 25 IU/kg. Open symbols represent the unloaded polymers as the control. Each data represents the mean  $\pm$  S.D. ( $n=6$ ).

effects or insulin absorption was observed following intestinal administration of insulin solutions [18]. Clearly, in all of the ILP formulations administered, a hypoglycemic effect concurrent with insulin absorption through the illeal mucosa was observed. In these

samples, insulin was released from the complexation gels and absorbed through the intestinal mucosa. No effects were observed using the control samples (polymer alone). Using the test conditions, no hypoglycemic effect or insulin absorption would be observed if insulin solutions were applied alone [18].

The pharmacokinetic parameters, based on the data of Fig. 7, are shown in Table 1. Notably, ILP II, which had already used for oral insulin delivery in our previous study, produced almost the same value of pharmacological availability and bioavailability of insulin as that in previous studies [18]. With respect to the comparison of hypoglycemia effect and insulin absorption, ILP II and III had similar pharmacological effects, particularly with respect to the calculated pharmacokinetic parameters including  $T_{max}$  and  $C_{max}$ . This is consistent with the in vitro release profiles, which were similar for ILP II and III. However, it is significant to note that ILP I, which exhibited the slowest in vitro release profile,  $T_{max}$  was increased by 5 min. This results from the slower rate of insulin release and absorption as observed in Figs. 6 and 7. Furthermore, the pharmacological bioavailability and bioavailability were greatest for ILP I. This is due to the fact that ILP I was the slowest releasing polymer.

For all of the ILP samples tested, the pharmaceutical bioavailability and bioavailability ranged from 4.6 to 7.4. In comparison, when insulin solutions were administered in intestinal mucosa in rats, the pharmacological bioavailability and absolute bioavailability was significantly less than 1% [18]. This is significant because it is evidence that complexation polymers are effective carriers for delivery of insulin in the upper small intestine as they provide for protection of insulin from the harsh environment of the GI tract

Table 1

Pharmacokinetic parameters following intestinal administration of ILP at a dose of 25 IU/kg in rats

	$C_{max}$ ( $\mu$ U/ml)	$T_{max}$ (min)	MRT ( $h^{-1}$ )	PA <sup>a</sup> (%)	$F^b$ (%)
ILP III	173.2 $\pm$ 33.7	10	0.677 $\pm$ 0.029	4.6 $\pm$ 1.4	4.6 $\pm$ 0.9
ILP II	225.3 $\pm$ 45.7	10	0.667 $\pm$ 0.070	5.2 $\pm$ 1.0	5.8 $\pm$ 0.9
ILP I	209.6 $\pm$ 92.3	15	0.799 $\pm$ 0.153	7.4 $\pm$ 2.1	6.2 $\pm$ 2.7

Each data represents the mean  $\pm$  S.D. ( $n=4$ ).

<sup>a</sup> Pharmacological bioavailability =  $(AUC_{ILP}/DOSE_{ILP}) / (AUC_{SC}/DOSE_{SC}) \times 100$ .

<sup>b</sup> Bioavailability =  $(AUC_{ILP}/DOSE_{ILP}) / (AUC_{SC}/DOSE_{SC}) \times 100$ .

but also aid in the absorption of the drug in the upper small intestine. These data agree with previous work where it has been established that P(MAA-g-EG) hydrogels are promising carriers for oral insulin delivery since the insulin due to (1) the pH/complexation responsive release behavior that provides for protection of the drug in the stomach and rapid release of the drug in the upper small intestine and (2) the absorption enhancing effect of the polymer [13, 16,18].

#### 4. Conclusions

In this study, the effects of solvent content during polymerization on the behavior and structure of pH responsive, complexation hydrogels has been evaluated. Gels prepared with greater amounts of solvent swelled to a greater degree and had a larger network mesh size. However, all of the polymers prepared had the necessary network structure to efficiently incorporate insulin (greater than 90%) into their pores. In the *in vitro* release studies, no insulin was released from any of the gels in the acidic media (simulating stomach conditions) but rapid release occurred in the higher pH solution (pH = 7.4), indicating the potential for drug release in the upper small intestine. The release rates in the higher pH solutions increased with increasing solvent fraction during polymerization. In the closed loop animal model, all of the materials provided for significant hypoglycemic effect and insulin absorption in the upper small intestine. The pharmacological effect was found to be dependent on the solvent reaction content. Gels prepared with the least amount of solvent provided for the greatest sustained release and bioavailability. It has been demonstrated that the efficacy of the complexation polymers for insulin delivery can be controlled by varying the network structure during the polymerization step.

#### Acknowledgements

This study was supported by the grant from the National Institutes of Health #7-R01-EB000246.

#### References

- [1] M. Thanou, J.C. Verhoef, P. Marbach, H.E. Junginger, Intestinal absorption of octreotide: *N*-trimethyl chitosan chloride (TMC) ameliorates the permeability and absorption properties of the somatostatin analogue *in vitro* and *in vivo*, *J. Pharm. Sci.* 89 (2000) 951–957.
- [2] Y. Onuki, M. Morishita, K. Takayama, S. Tokiwa, Y. Chiba, K. Isowa, T. Nagai, *In vivo* effects of highly purified docosa-hexaenoic acid on rectal insulin absorption, *Int. J. Pharm.* 198 (2000) 147–156.
- [3] T. Uchiyama, T. Sugiyama, Y.S. Quan, A. Kotani, N. Okada, T. Fujita, S. Muranishi, A. Yamamoto, Enhanced permeability of insulin across the rat intestinal membrane by various absorption enhancers: their intestinal mucosal toxicity and absorption-enhancing mechanism of *n*-lauryl-beta-D-maltopyranoside, *J. Pharm. Pharmacol.* 51 (1999) 1241–1250.
- [4] V. Agarwal, S. Nazzal, I.K. Reddy, M.A. Khan, Transport studies of insulin across rat jejunum in the presence of chicken and duck ovomucoids, *J. Pharm. Pharmacol.* 53 (2001) 1131–1138.
- [5] A. Yamamoto, T. Taniguchi, K. Rikyuu, T. Tsuji, T. Fujita, M. Murakami, S. Muranishi, Effect of various protease inhibitors on the intestinal absorption and degradation of insulin in rats, *Pharm. Res.* 11 (1994) 1496–1500.
- [6] E.A. Hosny, H.I. Al-Shora, M.M. Elmazar, Oral delivery of insulin from enteric-coated capsules containing sodium salicylate: effect on relative hypoglycemia of diabetic beagle dogs, *Int. J. Pharm.* 237 (2002) 71–76.
- [7] Y.H. Lee, B.A. Pery, S. Labruno, H.S. Lee, W. Stern, L.M. Falzone, P.J. Sinko, Impact of regional intestinal pH modulation on absorption studies of salmon calcitonin in beagle dogs, *Pharm. Res.* 16 (1999) 1233–1239.
- [8] S. Sakuma, N. Suzuki, R. Sudo, K. Hiwatari, A. Kishida, M. Akashi, Optimized chemical structure of nanoparticle as carriers for oral delivery of salmon calcitonin, *Int. J. Pharm.* 239 (2002) 185–189.
- [9] I. Ezpeleta, M.A. Arangoa, J.M. Irache, S. Stainmesse, C. Chabenat, Y. Popineau, A.M. Orecchioni, Preparation of *Ulex europaeus* lectin–gliadin nanoparticle conjugates and their interaction with gastrointestinal mucus, *Int. J. Pharm.* 191 (1999) 25–32.
- [10] M.A. Arangoa, G. Ponchel, A.M. Orecchioni, M.J. Renedo, D. Duchene, J.M. Irache, Bioadhesive potential of gliadin nanoparticle systems, *Eur. J. Pharm. Sci.* 11 (2000) 333–341.
- [11] D. Scherer, F.C. Mooren, R.K. Kinne, J. Kreuter, *In vitro* permeability of PBCA nanoparticle through porcine small intestine, *J. Drug Target.* 1 (1991) 21–27.
- [12] P. Jani, G.W. Halbert, J. Langridge, A.T. Florence, Nanoparticle uptake by the rat gastrointestinal mucosa: quantitation and particle size dependency, *J. Pharm. Pharmacol.* 42 (1990) 821–826.
- [13] A.M. Lowman, M. Morishita, M. Kajita, T. Nagai, N.A. Peppas, Oral delivery of insulin using pH-responsive complexation gels, *J. Pharm. Sci.* 88 (1999) 933–936.

- [14] A.M. Lowman, N.A. Peppas, Design of oral delivery systems for peptides and proteins using complexation graft copolymer networks, in: N.A. Peppas, D.J. Mooney, A.G. Mikos, L. Brannos-Peppas (Eds.), *Biomaterials, Carriers for Drug Delivery and Scaffolds for Tissue Engineering*, AIChE, New York, 1997, pp. 21–23.
- [15] A.M. Lowman, N.A. Peppas, Analysis of the complexation/decomplexation phenomena in polyelectrolyte networks, *Macromolecules* 30 (1997) 4659–4965.
- [16] M. Morishita, A.M. Lowman, K. Takayama, T. Nagai, N.A. Peppas, Elucidation of the mechanism of incorporation of insulin in controlled release systems based on complexation polymers, *J. Control. Release* 81 (2002) 25–32.
- [17] M. Torres-Lugo, M. Garcia, R. Record, N.A. Peppas, Physicochemical behavior and cytotoxic effects of p(methacrylic acid-g-ethylene glycol) nanoparticles for oral delivery of proteins, *J. Control. Release* 80 (2002) 197–205.
- [18] M. Morishita, J.I. Joseph, M.C. Torjman, C. Munsick, T. Goto, K. Takayama, N.A. Peppas, A.M. Lowman, Mucosal insulin delivery systems based on complexation polymer hydrogels: effect of particle size on insulin enteral absorption, *J. Control. Release* (submitted for publication).
- [19] K.A. Berchtold, L.G. Lovell, J. Nie, B. Hacioglu, C.N. Bowman, The significance of chain length dependent termination in cross-linking polymerization, *Polymer* 42 (2001) 4925–4929.
- [20] J.E. Elliott, J.W. Anseth, C.N. Bowman, Kinetic modeling of the effect of solvent concentration on primary cyclization during polymerization of multifunctional monomers, *Chem. Eng. Sci.* 56 (2001) 3173–3184.
- [21] P.J. Flory, *Principles of Polymer Chemistry*, Cornell University Press, Ithaca, NY, 1953.
- [22] R.G. Treloar, *The Physics of Rubber Elasticity*, Oxford Univ. Press, Oxford, 1958.